iFEM Implementation on a Rotating Shaft for Imbalance Identification

EMANUELE PETRICONI, LIBERO LUCII, MARCO GIGLIO and CLAUDIO SBARUFATTI

ABSTRACT

Structural Health Monitoring (SHM) is crucial for ensuring the safety and reliability of rotating machinery. In rotating shafts, structural damage can affect force distribution and alter dynamic behavior. This study conducts a preliminary numerical investigation into the application of the inverse Finite Element Method (iFEM) for rotor monitoring. Based on Euler-Bernoulli beam theory, the iFEM algorithm reconstructs the full three-dimensional deformation field through beam elements of inverse fi nite ñth-order formulation. Static and dynamic Finite Element Method (FEM) simulations assess the accuracy of the methodology under varying loading and boundary conditions. To simulate real-world sensor inaccuracies, Gaussian noise is introduced into the strain data, replicating measurement uncertainties typical of Fiber Bragg Grating (FBG) optical sensors. Results demonstrate the strong iFEM capability to capture deformation patterns, paving the way for iFEM real-time monitoring of a rotating shaft. Its sensitivity to structural changes highlights its suitability for predictive maintenance and fault diagnostics in rotating machinery. This study lays the groundwork for further research into iFEM-based SHM implementations, supporting research advancements and new industrial applications.

INTRODUCTION

Rotating machinery plays a crucial role in various industrial fields by transmitting motion and forces within mechanical systems. Unexpected failures can lead to costly downtime and critical safety concerns, traditionally addressed through schedule-based maintenance. While effective in preventing abrupt failures, this approach often results in early component replacement and elevated operational and maintenance (O&M) costs. To enhance economic sustainability, research has shifted toward automated, condition-based maintenance strategies supported by Structural Health Monitoring (SHM) technologies. By leveraging periodic or continuous monitoring of structural and environmental parameters, SHM facilitates early anomaly detection and extends component lifespan while reducing O&M costs.

Petriconi Emanuele, PhD Student, Email: emanuele.petriconi@polimi.it, Department of Mechanical Engineering, Politecnico di Milano, Milan, MI, Italy

SHM methodologies are generally classified into data-driven [1] and model-based [2] approaches. Data-driven techniques rely solely on previously acquired data, leveraging machine learning and statistical pattern recognition algorithms to detect anomalies, representing black-box models without any relation to the physics of the problem. Conversely, model-based methods integrate physics-based models, enhancing accuracy and interpretability but requiring detailed structural knowledge and computational resources. Among the various SHM techniques, vibration-based methods [3] and the Wavelet Finite Element Method (WFEM) [4] are widely adopted due to their cost-effectiveness and ease of implementation. Modal analysis [5] and vibroacoustic techniques [6] also significantly contribute to the field. Nonetheless, accelerometers installed on the supports of a rotating shaft inevitably capture a superposition of vibrations originating from the shaft and other surrounding mechanical components of the structure. To enhance the accuracy of vibration measurements, one potential approach involves mounting accelerometers directly on the rotating shaft. However, this solution introduces several technical challenges, including the non-negligible influence of the sensor mass on the dynamic behavior of the system and the inherent complexity of transmitting electrical signals from the rotating shaft to a stationary data acquisition system in high-rotational environments. In this context, recent advances in sensor technology enable real-time shape sensing, allowing for full-field displacement reconstruction based on in situ strain measurements. To address the above-mentioned challenges, optical strain sensors are commonly installed on the structure of interest. These sensors are characterized by an extremely low mass, resulting in a negligible effect on the dynamic behavior of the system when compared to the aforementioned accelerometers. Furthermore, the transmission of optical signals from the rotating shaft to the stationary data acquisition system is more compact thanks to multiplexing capabilities. Techniques in this area include basis function methods [7], mode-shape reconstruction [8], and beam theory-based approaches [9]. However, many shape-sensing methods require prior knowledge of material and load conditions. The inverse Finite Element Method (iFEM) addresses this limitation, offering accurate, robust displacement reconstruction with minimal prior information. Unlike data-driven methods, which rely entirely on previous data, iFEM benefits from the integration of physics-based models. This approach isolates the response of the shaft itself, without interference from the surrounding components. Originally developed by Tessler and Spangler for shear-deformable plate and shell structures [10], iFEM uses a least-squares variational principle to reconstruct full-field displacements from surface strain measurements. Further developments adapted iFEM for truss and beam structures using Timoshenko [11] and Euler-Bernoulli [12] theories. Pre-extrapolation methods—including polynomial functions, smoothing element analysis, physics-based models, and Gaussian process interpolation—have improved reconstruction in sensor-limited scenarios.

This research covers the first feasibility assessment for iFEM implementation on a rotating shaft, employing Euler-Bernoulli beam theory and the 0^{th}-order inverse element formulation. The study presents an overview of the methodology employed, introduces the case study under investigation, and discusses numerical results regarding the method's accuracy and implementability in real-world scenarios. Finally, a discussion on key findings, limitations, and future research developments is presented, emphasizing the necessity for an experimental validation to confirm the performances obtained numerically.

METHODOLOGY

The proposed methodology employs a bidimensional iFEM formulation based on Euler-Bernoulli beam theory and 0^{th}-order element formulation to reconstruct the 3D deformed shape of a rotating shaft subjected to an unbalanced mass fixed to its external surface. The iFEM is a computational technique that uses in situ strain measurements to reconstruct the beam's displacement field, allowing the calculation of internal strains and stresses. The method applies a variational principle, minimizing the least-squares error between experimentally measured strains $\mathbf{e}^{\varepsilon}$ and analytical strains $\mathbf{e}(\mathbf{u})$. This approach leads to the development of a functional, $\Phi(\mathbf{u}) = \|\mathbf{e}(\mathbf{u}) - \mathbf{e}^{\varepsilon}\|^2$ which quantifies the difference between the measured and predicted strains, and is minimized to obtain the best approximation of the displacement field. In this case, analytical strains are derived from the Euler-Bernoulli beam theory, which is well-suited for modelling an elastic, homogeneous, and isotropic shaft. It involves the theoretical assumption that the shaft cross-section remains flat and perpendicular to the main axis during deformation, which implies that the shaft deforms through bending and stretching, without shear deformation or torsion. The shaft's displacement field is defined by five kinematic variables: the transverse displacements u and v along the x- and y-axes, respectively; the longitudinal displacement w along the z-axis; and the section rotations φ_x and φ_y, around the x- and y-axes, respectively. These displacements define the beam's deformation in space and time, and are governed by the beam's geometry and material properties, such as Young's modulus (E), shear modulus (G), and Poisson's ratio (ν). Subsequently, the corresponding strain field is defined by the axial strain $\varepsilon_{z0} = \frac{dw}{dz}$, and the curvatures $\chi_x = -\frac{d^2v}{dz^2}$ and $\chi_y = \frac{d^2u}{dz^2}$ along the x- and y-axes respectively. The axial strain accounts for elongation or compression along the shaft's length, while the curvatures represent the beam's bending behavior. Internal forces and moments resulting from the deformations can then be fully described.

Similar to the direct Finite Element Method (dFEM), the entire structure of interest is discretized into finite elements (see Figure 1). For each element, the displacement is approximated as a combination of nodal Degrees Of Freedom (DOF) and appropriately chosen shape functions. The iFEM method allows for the computation of the overall structure's displacement field by summing the contributions from all elements, resulting in a system of equations that can be solved after specifying the problem's boundary conditions. Two types of elements are commonly used in iFEM: 0^{th}-order and 1^{st}-order

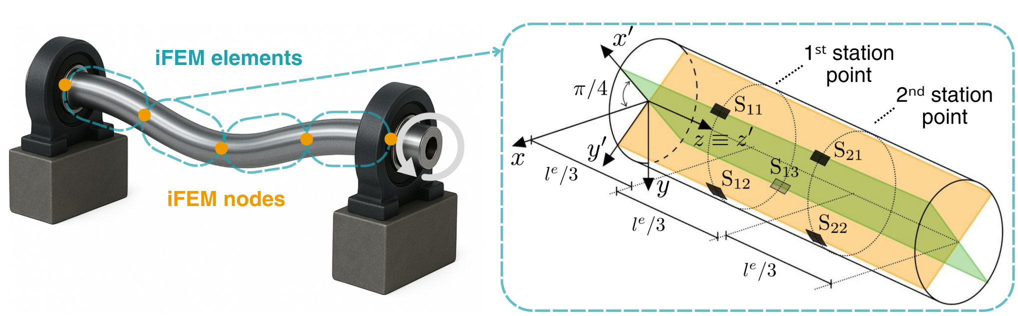

Figure 1. Schematic representation of iFEM discretization on a rotating shaft (left) and the positioning of sensors and station points for strain measurement (right).

elements. The 0^{th}-order element, characterised by two nodes at the extremes, is suitable for modelling concentrated forces and moments at nodes. The displacement field for this element is assumed to have linear variation for the curvatures and constant axial deformation. This results in a total of 10 DOF for each element, making it computationally efficient, though less accurate for more complex deformations. On the other hand, the 1^{st}-order element is characterized by three nodes (with one located at the center of the element) and assumes quadratic variation for the curvatures. This element has 14 DOF and provides a more accurate modelling of the displacement field, while it requires more computational resources. In the presented work, the selection of 0^{th}-order iFEM element formulation depends on a trade-off between the required accuracy, computational efficiency, and the needed number of strain sensors. For each beam inverse element, a minimum of 5 strain evaluations are required to determine the axial strain and bending curvatures within the element. Figure 1 illustrates the selected placement of station points along the element's length, as well as the positioning of sensors at each station point. The two station points are located at $\frac{l^e}{3}$ and $\frac{2l^e}{3}$, with l^e representing the element length. The 0^{th}-order formulation reduces computational complexity while providing sufficiently accurate deformation reconstruction, especially when distributed forces are small relative to concentrated ones. In cases of intensive distributed forces, higher-order elements may be required, particularly when using a coarse discretization.

The 3D shaft deformed shape is reconstructed by solving two independent bidimensional problems in the perpendicular planes $x'z'$ and $y'z'$ belonging to the local reference system $x'y'z'$ (see Figure 1). Subsequently, the two resulting deformations are combined using the Pythagorean theorem, and the outcome is transformed to the global reference system xyz with the application of appropriately constructed rotational matrices, which depend on the instantaneous angular position of the shaft during its rotation.

In this preliminary feasibility assessment phase, the proposed methodology is tested on a rotating shaft Finite Element Method (FEM) simulations, from which the necessary data for the iFEM method development are derived. The target FEM-based shaft axis deformation $(\cdot)_{\mathrm{t}}$ is then compared with the one reconstructed using the iFEM method $(\cdot)_{\mathrm{iFEM}}$, which relies on discrete surface strain data extracted from numerical simulations.

CASE STUDY

To assess the effectiveness of the proposed methodology, a case study was conducted on several FEM simulations of a rotating shaft subjected to an external surface-mounted unbalanced mass. The shaft is modeled as a solid steel cylinder with a diameter of 32 mm and a length of 1226 mm. The selected mass values, ranging from 10 to 60 grams, were informed by prior research activities, which investigated the unbalanced forces induced on a rotating shaft as a result of a projectile's ballistic impact [13]. The shaft is supported at both ends. The FEM simulations cover both static and dynamic cases, considering various boundary conditions and loading scenarios such as pinned-pinned and clamped-clamped shafts, as well as different application points and intensities of the unbalanced mass. Mesh generation for FEM simulations is critical for accurate results. Moreover, given that Abaqus computes strain at integration points, surface strain data are extrapolated using methods such as node averaging, skin layers, or integration point mapping. The accuracy of the iFEM-based methodology is evaluated by comparing the reconstructed shaft axis deformation with the target one, using three key metrics:

- **Deformation Error E_1:** which measures the proportional discrepancy in displacement magnitude at each axial position z_i along the shaft, highlighting global variations compared to the target values:

$$E_1(z_i) = \frac{\sqrt{x_t(z_i)^2 + y_t(z_i)^2} - \sqrt{x_{iFEM}(z_i)^2 + y_{iFEM}(z_i)^2}}{\sqrt{x_t(z_i)^2 + y_t(z_i)^2}} \tag{1}$$

  The focus is on the maximum value computed over all axial positions z_i along the shaft, denoted as $E_{1,\text{max}}$.

- **Angular Error E_2:** which measures the proportional error in angular displacement α, providing insight into discrepancies in the curvature-induced rotation along the shaft:

$$E_2(z_i) = \frac{\alpha_t - \alpha_{\text{iFEM}}}{\alpha_t} \tag{2}$$

  The focus is on the maximum value computed over all axial positions z_i along the shaft, denoted as $E_{2,\text{max}}$.

- **Maximum Displacement Error E_3:** which measures the proportional difference in peak displacement d:

$$E_3 = \frac{d_t - d_{\text{iFEM}}}{d_t} \tag{3}$$

The iFEM method's robustness and accuracy are evaluated by varying the number of elements in the shaft's discretization. To assess sensitivity to measurement uncertainty, Gaussian noise with zero mean and variance 1.7×10^{-6}, representative of typical optical fiber strain sensor error, is introduced. This allows for a robustness assessment of the reconstruction process under realistic sensing conditions. Moreover, to further reduce sensor requirements, the possibility of assuming null axial strain is evaluated, reducing the required number of sensors for each inverse element to 4. Lastly, the effects of distributed forces and the influence of varying strain sensor lengths are also examined.

RESULTS

This study validates the proposed iFEM methodology for reconstructing the 3D deformed shape of a rotating shaft subjected to various loading conditions through output strains obtained from FEM simulations in Abaqus. A double-pinned shaft with a midpoint load along the y-axis approximately 100 N, serves as the primary case study, referred to as *Case 1*. The study first demonstrates that the dynamic behavior of a rotating shaft can be approximated as a series of static problems from the displacement point of view, each corresponding to a specific time instant of the simulation. The influence of the mode shapes results to be negligible with respect to the deformation induced by the imbalances. This assumption is not valid for vibration-based monitoring techniques.

The iFEM reconstruction is performed using different mesh refinement levels, and the results are compared to the deformation obtained from FEM simulations in Abaqus.

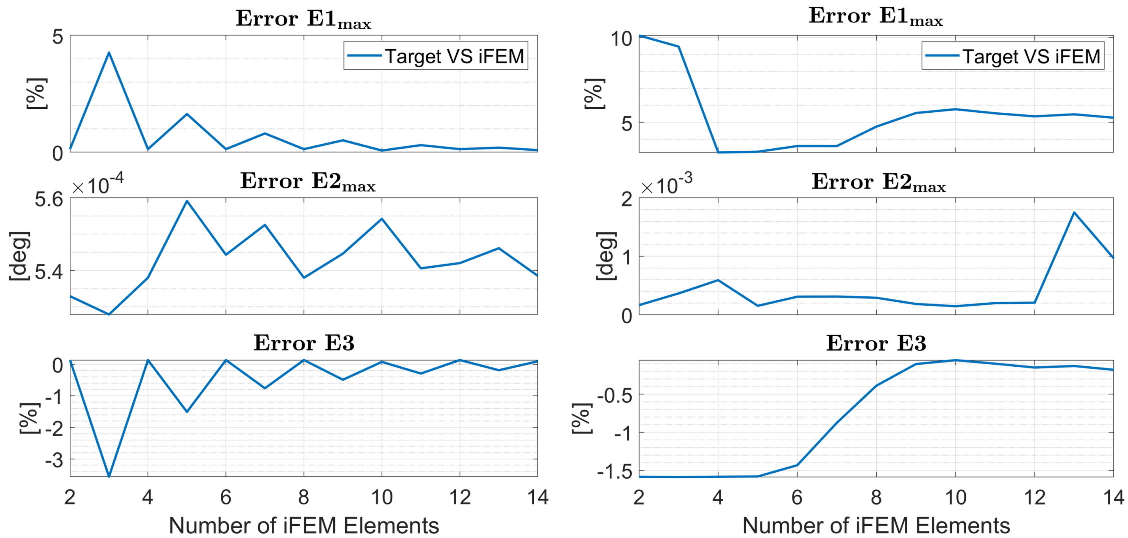

Figure 2. Key error trends between target FEM-based shaft axis deformation and iFEM-reconstructed solution as a function of mesh refinement for *Case 1* (right) and *Case 2* (left).

Finer discretizations generally lead to higher accuracy, but diminishing returns are observed when the load application point does not overlap with an iFEM node. However, as the number of iFEM elements increases, this influence becomes negligible, and the error trends stabilize (see Figure 2 (right)). Additionally, in *Case 2*, a 100 N load is applied at a distance of $L/10$ from one shaft support. Similar oscillatory trends to *Case 1* are observed for error metrics; however, results show a local minimum at 11 elements (see Figure 2 (left)). In this specific condition, the applied concentrated load precisely aligns with a node of the iFEM mesh.

Results indicate that, as in real-world scenarios load application points are generally unknown, the number of iFEM nodes significantly influences the iFEM reconstruction accuracy. Therefore, a sufficiently fine discretization should be chosen to ensure a proper trade-off between reconstruction accuracy and computational cost.

Additionally, the accuracy of the iFEM reconstruction method is found to be robust across different scenarios, including gravitational and centrifugal distributed loads. The study also examines the impact of varying the strain sensor length and reducing the number of strain sensors per inverse finite element. Regarding the former, varying the strain sensor length—typically ranging from 5 mm to 10 mm—does not show any significant differences in the key error metric results, as the sensor length remains small relative to both the total shaft length and the expected strain curvature along the shaft axis. Regarding the latter, it is found that configurations with 5 and 4 strain sensors per inverse element achieve comparable results, confirming the negligibility of the axial strain. Finally, noise is added to the strain measurements obtained from Abaqus simulations to assess its effect on the accuracy, precision, and robustness of the iFEM reconstruction methodology. This procedure is illustrated in Figure 3 for *Case 1*. Results show an increase in error metrics. This effect is particularly pronounced in cases with low strain values. In scenarios with greater deformations and higher strain values, the relative error increase is less significant, as the improved signal-to-noise ratio mitigates its impact.

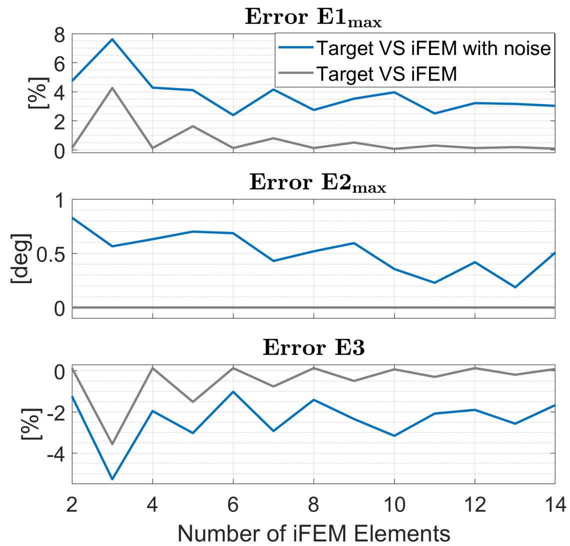

Figure 3. Key error trends between target FEM-based shaft axis deformation and iFEM-reconstructed solution as a function of mesh refinement for *Case 1* (right), shown both in the absence and presence of added measurement noise.

Results confirm that the iFEM methodology, based on Euler-Bernoulli beam theory and 0^{th}-order formulation, is an effective tool for reconstructing the 3D deformed shape of a rotating shaft under different scenarios.

CONCLUDING REMARKS

This study presents the preliminary assessment for the iFEM implementation on a rotating shaft. The performance of the proposed approach is assessed by comparing the obtained results with a high-fidelity model. Static and dynamic simulations are performed considering different conditions to evaluate the robustness and applicability of the developed methodology. The iFEM reconstruction accuracy is tested under different discretization levels, where finer meshes generally yield higher precision. However, exceptions may occur in specific cases, particularly when the applied load coincides with an iFEM node. This implies that the selection of the number of inverse finite elements is problem-specific. Furthermore, the study demonstrates that the dynamic behaviour of a rotating shaft can be effectively approximated as a sequence of static problems from the displacement point of view, thereby enabling the proposed methodology to be applied without loss of accuracy. The influence of the mode shapes results to be negligible with respect to the deformation induced by the imbalances. A consistent accuracy across varying boundary conditions and applied loads is found. The robustness of the approach is confirmed also under distributed loading conditions and in the presence of measurement noise, highlighting the effectiveness across diverse operational environments. Future research activities will focus on the implementation and experimental validation of the proposed methodology on a dedicated test rig, providing further insights into its real-world applicability. Additionally, the integration of advanced data processing techniques could enhance the adaptability and resilience of the reconstruction method. Another promising direction is the use of virtual sensors to extend the methodology. Moreover, diagnosis can be systematically conducted by comparing real-time displacement reconstructions with reference models obtained under undamaged conditions. In conclusion, this study underlines the potential of iFEM-based displacement reconstruction for SHM applications in rotating machinery, presenting a novel methodological contribution to this engineering domain. It offers a thorough assessment of the software's feasibility, paving the way for advancements in real-time SHM and predictive maintenance strategies for rotating machinery.

REFERENCES

1. Yuen, K.-V. and G. A. Ortiz. 2017. "Outlier detection and robust regression for correlated data," *Computer Methods in Applied Mechanics and Engineering*, 313:632–646.
2. Concli, F., L. Pierri, and C. Sbarufatti. 2021. "A model-based SHM strategy for gears—development of a hybrid FEM-analytical approach to investigate the effects of surface fatigue on the vibrational spectra of a back-to-back test rig," *Applied Sciences*, 11(5):2026.
3. Chatterton, S., P. Borghesani, P. Pennacchi, and A. Vania. 2015. "Monitoring of the Damage in Rolling Element Bearings," in J. K. Sinha, ed., *Vibration Engineering and Technology of Machinery*, Springer International Publishing, Cham, ISBN 978-3-319-09918-7, pp. 977–986.
4. Xiang, J., X. Chen, Q. Mo, and Z. He. 2007. "Identification of crack in a rotor system based on wavelet finite element method," *Finite Elements in Analysis and Design*, 43(14):1068–1081.
5. Mironov, A., P. Doronkin, A. Priklonsky, and I. Kabashkin. 2016. "Structural health monitoring of rotating blades on helicopters," *Aviation*, 20(3):110–122.
6. Burdzik, R., Ł. Konieczny, and P. Folega. 2014. "Structural health monitoring of rotating machines in manufacturing processes by vibration methods," *Advanced Materials Research*, 1036:642–647.
7. Kim, H.-I., L.-H. Kang, and J.-H. Han. 2011. "Shape estimation with distributed fiber Bragg grating sensors for rotating structures," *Smart Materials and Structures*, 20(3):035011.
8. Bogert, P., E. Haugse, and R. Gehrki. 2003. "Structural shape identification from experimental strains using a modal transformation technique," in *44th AIAA/ASME/ASCE/AHS/ASC Structures, Structural Dynamics, and Materials Conference*, p. 1626.
9. Ko, W. L., W. L. Richards, and V. T. Fleischer. 2009. "Applications of Ko displacement theory to the deformed shape predictions of the doubly-tapered Ikhana Wing," Tech. rep.
10. Tessler, A. and J. L. Spangler. 2005. "A least-squares variational method for full-field reconstruction of elastic deformations in shear-deformable plates and shells," *Computer methods in applied mechanics and engineering*, 194(2-5):327–339.
11. Gherlone, M., P. Cerracchio, M. Mattone, M. Di Sciuva, and A. Tessler. 2012. "Shape sensing of 3D frame structures using an inverse finite element method," *International Journal of Solids and Structures*, 49(22):3100–3112.
12. Savino, P. 2019. "Shape sensing with inverse finite element method for slender structures," *Structural Engineering and Mechanics, An Int'l Journal*, 72(2):217–227.
13. Panagiotopoulou, V., L. Brancato, E. Petriconi, M. U. G. M. Baldi, Andrea, and C. Sbarufatti. 2025. "Comparative study on ballistic impact detection in helicopter transmission shafts using NARX and LSTM models," *Applied Intelligence*, 55:264.